IJE TRANSACTIONS B: Applications Vol. 27, No. 5, (May 2014) 793-802

International Journal of Engineering

Journal Homepage: www.ije.ir

An Analytical Model for Flame Propagation through Moist Lycopodium Particles with Non-unity Lewis Number

M. Bidabadi [a], S. A. Mostafavi* [b], F. Faraji Dizaji [a], H. Beidaghy Dizaji [a]

[a] *Department of Mechanical Engineering, Iran University of Science and Technology, Tehran, Iran*
[b] *Department of Mechanical Engineering, Faculty of Engineering, Arak University, Iran*

PAPER INFO

Paper history:
Received 21 November 2012
Received in revised form 15 September 2013
Accepted 21 January 2014

Keywords:
Analytical Model
Lycopodium particle
Moisture content
Lewis number
Flame Temperature
Burning Velocity

ABSTRACT

In this investigation, the structure of one-dimensional flame propagation in uniform cloud of volatile organic particles has been analyzed in which the structure of flame is divided into three zones. The first zone is preheat zone which is divided into three subzones itself. In the first subzone (heating), particle cloud is heated until the moist particles reach to vaporization temperature (water vapor). In the next subzone (drying), particle moisture comes out, and in the final subzone the pyrolysis phenomenon takes place. The second zone is the reaction zone, and the last one is the post-flame zone. In this research, an analytical method is used in order to solve the governing equations of particle cloud combustion in aforementioned zones. The overall investigation of this study leads to a non-linear burning velocity correlation. Consequently, the results show that a decrease in particle moisture content or an increase in equivalence ratio (φ_u) or Lewis number causes to increase in moisture evaporation and devolatization rates, and consequently both flame temperature and burning velocity increase

doi: *10.5829/idosi.ije.2014.27.05b.16*

1. INTRODUCTION

In recent years, many discussions about completion of fossil fuel resources have been negotiated. In many countries, fossil fuels are the main energy source of human activities. These resources can afford human necessity just for a few decades, thus finding new replacements for energy sources is a challenging issue for energy security. Investigations to produce energy from biomass and municipal solid waste have been done by many researchers [1-4]. Biomass is presently estimated to contribute of the order 10–14% of the world's energy supply [5]. It is notable that biomass consumption does not have any by-products like CO_2 generation [6, 7]. Biomass has low energy density, therefore transportation of these fuels to power plants isn't economical. However, small scale biomass conversion system is suitable for local usage. The Stirling engine is one of the best available technologies for small-scale power production from biomass. To achieve a reliable model for biomass combustion, research on organic particles cloud is necessary.

On the other hand, more than 70% of dusts processed in industry such as wood processing and storage; grain elevators, bins and silos; flour and feed mills; starch or candy production; spice sugar and cocoa production and storage; coal handling or processing area are combustible [8]. Understanding of burning mechanism of organic particles may help us to prevent dust explosion and its hazards [9]. The history of the industrial development has been punctuated by a number of hazardous explosions with a frequency and severity level increasing in proportion of the spreading of process industry [10].

The most important dust explosions happen in coal mining industry. These accidents spread little by little throughout the whole industry field. It commonly admitted that one dust explosion occurs in each industrialized country every day [11].

A dust explosion is likely to occur when a finely divided combustible solid (in practice, the mean

*Corresponding Author Email: a-mostafavi@araku.ac.ir (S. A. Mostafavi)

diameter of the particles should not exceed 1 mm) happens to be dispersed as a cloud in air (with a typical mass loading between 10 and 1000 grams of dust per cubic meter or cloud), and when an appropriate ignition source (hot body, flame, electrical or mechanical spark, etc.) is activated inside the mixture. The heat evolved from the ignition source initiates the combustion of the particles located in the vicinity of the ignition point. These particles act themselves as an ignition source for the adjacent slabs of the mixture so that a 'combustion zone' is allowed to propagate without additional input of energy throughout the cloud. This 'combustion zone' has generally a finite thickness and is called the 'flame' [12].

Experimental researches show that moisture content and particle size have great impact on dust explosion. According to previous investigations, some definitions were characterized, like MIT point. The lowest temperature at which ignition occurs is characterized as 'minimum ignition temperature' (MIT). MIT increases with the presence of moisture in dust cloud, but it decreases by decreasing the particle size and increasing in volatile matter, oxygen concentration, and thickness of dust layer [10].

Experimental evidence gathered over the last two decades support the idea that the basic flame propagation mechanism in dust clouds has a general similarity with premixed gaseous flames [11]. Beside this, they have differences, a dust particle must first volatilize before catching fire [9]. In fact, organic dusts combustion starts after a devolatilization process [13, 14] in which any different particle in material and size behaves distinctively. In some cases like coal when the particle is exposed to heat sources, it is cracked to gas, liquid and solid phases that are named respectively gas, tar and char. In this study, it is assumed that lycopodium particles particle is only converted to gas.

The rate and the extent of flame propagation depend on factors such as nature of dust, dust particle size, and nature of combustion byproducts. Dust combustion is a complex phenomenon in the sense that it involves simultaneous momentum, energy, and mass transport in a reactive multi-phase system [15].

In this article an analytical, approach has been used to evaluate the flame characteristics, and finally the effect of some important parameters such as moisture content, particle number density and Lewis number on the flame characteristics has been investigated.

2. GOVERNING EQUATION

A model is developed to describe steady, one-dimensional, planar flame propagation in a combustible mixture consisting of uniformly distributed moist volatile fuel particles in air. The initial number density of the moist particles, n_u (number of particles per unit volume) and the initial radius r_u, are presumed to be known. All external forces including gravitational effects are assumed to be negligible. Other approximations introduced are that diffusion caused by pressure gradient is negligible, Soret and Dufour effects are negligible, and heat transport by radiation is negligible.

In previous researches [16-19], it has been assumed that lycpodium particles are dry, however in this work, it is assumed that they contain moisture and final product of thermal degradation is mainly methane. Devolatilization rate of moist particle has two steps, namely moisture evaporation (drying), and volatile evaporation [16, 20]. The kinetics of pyrolysis and the kinetic of drying are expressed respectively by:

$$w_{pyr} = 4\pi A n_s r^2 (T - T_u)^n \quad (1)$$

$$w_{dry} = 4\pi A' n_s r^2 (T - T_u)^n \quad (2)$$

Since large portion of gaseous fuel is methane, the gas properties are considered the same as methane. Since the fuel is burnt in air oxidizer bed, the combustion products are assumed to be CO_2 and H_2O. Reaction occurs in thin zone O(ε) whereas preheat and post flame zones have considerable length. This assumption is based on high Zeldovich number and ε is defined as a reciprocal of Zeldovich number. The flame structure is divided into to three zones: preheat zone, reaction zone and post flame zone. The Zeldovich number, which is presumed to be large, is defined as:

$$Ze = \frac{E(T_f - T_u)}{RT_f^2} \quad (3)$$

Here the subscripts f and u denote conditions in the flame and the ambient reactant stream, respectively.

It is assumed that internal resistance versus external resistance is negligible (Bi=0) since particles are micro-scale. From this assumption, it is concluded that heating, drying and volatile evaporation processes do not occur simultaneously. To observe aforementioned processes individually, preheat zone itself is divided into three subzones: heating, drying and volatile evaporation. In each subzone of preheat zone, different reactions take place; particles in heating subzone are heated from ambient temperature T=300K to reach T=373K. In drying subzone, the moisture content of particles is evaporated, and finally in volatile evaporation subzone, volatile evaporation starts and particle shrinks to become a small fraction of its initial size. Figure 1 shows a schematic illustration of the presumed flame structure.

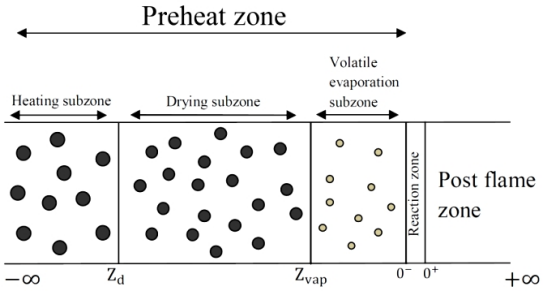

Figure 1. The flame structure of dust particles

General mass conservations, organic particles conservation, gas phase conservations equations along with energy conservations formulate the physical phenomena in solid particle combustion. State equation of gas phase mixture is used to close the equations in condition of atmospheric combustion.

The governing equations in this problem are nonlinear [16] which can be transformed into a linear form by introducing an independent variable x that is related to the spatial coordinate x' as:

$$x = \int_0^{x'} \left(\frac{\rho}{\rho_u} \right) dx' \tag{4}$$

➢ Mass conservation:

$$\rho v = cte \tag{5}$$

➢ Energy conservation:

$$\rho v C \frac{dT}{dx} = \lambda_u \frac{d^2T}{dx^2} + w_F \frac{\rho_u}{\rho} Q - w_{pyr} \frac{\rho_u}{\rho} Q_{pyr} \times H\left(x - x_{vap}\right) - w_{dry} \frac{\rho_u}{\rho} Q_{dry} \times H\left(x - x_d\right) \tag{6}$$

λ is heat conductivity, w_F gaseous fuel consumption rate, w_{pyr} organic particles devolatilization rate, w_{dry} moisture evaporation rate, Q the heat released from combustion, Q_{pyr} the heat absorbed by particles for devolatilization, Q_{dry} the heat required for drying and C heat capacity of mixture, and finally H the heavy side function.

➢ Gaseous fuel conservation:

$$\rho v \frac{dY_F}{dx} = \rho_u D_u \frac{d^2Y_F}{dx^2} - w_F \frac{\rho_u}{\rho} + w_{pyr} \frac{\rho_u}{\rho} \times H\left(x - x_{vap}\right) \tag{7}$$

In the above equation, Y is mass fraction and D mass difiusion coefficient.

➢ Equation of state

$$\rho T = cte \tag{8}$$

➢ Mass conservation of solid organic particles:

$$\rho v \frac{dY_S}{dx} = -w_{dry} \frac{\rho_u}{\rho} \times H\left(x - x_d\right) - w_{pyr} \frac{\rho_u}{\rho} \times H\left(x - x_{vap}\right) \tag{9}$$

The heat capacity of mixture C is the combined heat capacity of the gas C_p and the particles C_s, can be evaluated from the expression:

$$C = C_p + \frac{4\pi \left(r^3 C_s \rho_s n_s\right)}{3\rho} \tag{10}$$

➢ Boundary conditions are:

$$\begin{aligned} &\text{At: } x = -\infty \qquad T = T_u \, Y_s = Y_{Fu} \, Y_F = 0 \\ &\text{At: } x = +\infty \qquad T = Y_b \, Y_F = finite \end{aligned} \tag{11}$$

3. NONDIMENSIONALIZATION OF GOVERNING EQUATION

These parameters are used to nondimensionalize the governing equations:

$$\theta = \frac{(T - T_u)}{(T_f - T_u)} \qquad y_F = \frac{Y_F}{Y_{Fc}} \qquad y_s = \frac{Y_s}{Y_{Fc}}$$
$$m = \frac{\rho v}{\rho_u v_u} \qquad Z = \frac{\rho_u v_u C}{\lambda_u} x \qquad Z = \frac{\lambda}{\rho_u D_u C} \tag{12}$$

In the above equation, T_f is flame the temperature and Y_{Fc} is defined as:

$$Y_{Fc} \, Q = C\left(T_f - T_u\right) \tag{13}$$

Finally, these dimensionless quantities are defined:

$$\omega_F = \frac{\lambda_u w_F}{\left(\rho_u V_u\right)^2 C Y_{Fc}}$$
$$y_s = \frac{4\pi n_s \rho_s r^3}{3\rho Y_{Fc}}$$
$$q_1 = \frac{Q_{dry}}{Q} \qquad q_2 = \frac{Q_{pyr}}{Q} \tag{14}$$
$$\gamma_1 = \frac{4.836 \; A' n_u^{1/3} \lambda_u \left(T_d - T_u\right)^n}{V_u^2 \rho_u^{4/3} C Y_{Fc}^{1/3} \rho_s^{2/3}}$$
$$\gamma_2 = \frac{4.836 \; A n_u^{1/3} \lambda_u \left(T_f - T_d\right)^n}{V_u^2 \rho_u^{4/3} C Y_{Fc}^{1/3} \rho_s^{2/3}}$$

In the above equations, V_u is burning velocity of flame. q_2 has negligible quantity (close to zero) which means heat release from reaction is greater than heat absorbed by particles for devolatilization. Hence, q_1 is vanished in the next analysis step. In the same way, q_1 is supposed to be negligible to solve the conservation equations analytically, but in the resumption, the effect of moisture evaporation is added to the solution.

$$m\frac{d\theta}{dZ}=\frac{d^2\theta}{dZ^2}+\omega_F\frac{\rho_u}{\rho}$$
$$m\frac{dy_F}{dZ}=\frac{1}{Le}\frac{d^2y_F}{dZ^2}+\gamma_2 y_s^{\frac{2}{3}}\theta^n\times H(Z-Z_{vap})-\omega_F\frac{\rho_u}{\rho} \quad (15)$$
$$m\frac{dy_s}{dZ}=-\gamma_1 y_s^{\frac{2}{3}}\theta^n\times H(Z-Z_d)-\omega_F\frac{\rho_u}{\rho}-\gamma_2 y_s^{\frac{2}{3}}\theta^n\times H(Z-Z_{vap})$$

It is presumed that m=1, in this case we replace θ with θ° and thus dimensionless equations yield to:

$$\frac{d\theta^0}{dZ}=\frac{d^2\theta^0}{dZ^2}+\omega_F\frac{\rho_u}{\rho}$$
$$\frac{dy_F}{dZ}=\frac{1}{Le}\frac{d^2y_F}{dZ^2}+\gamma_2 y_s^{\frac{2}{3}}\theta^{0n}\times H(Z-Z_{vap})-\omega_F\frac{\rho_u}{\rho} \quad (16)$$
$$\frac{dy_s}{dZ}=-\gamma_1 y_s^{\frac{2}{3}}\theta^{0n}\times H(Z-Z_d)-\gamma_2 y_s^{\frac{2}{3}}\theta^{0n}\times H(Z-Z_{vap})$$

4. FLAME STRUCTURE ANALYSIS

Now, the above equations are solved in each zone by appropriate assumption to analyze the problem and evaluate the flame characteristics.

4. 1. Preheat Zones (-∞<Z<0) In the asymptotic solution (ε→0), reaction term can be neglected, because in preheat zone particles devolatilize and formed gaseous fuel without any reaction. Energy equation and boundary conditions are:

$$Z=0\rightarrow\theta^0=1,\quad Z=-\infty\rightarrow\theta^0=0 \quad (17)$$

By solving the above equation, the nondimensional temperature field is:

$$\theta^0=\exp(Z),\ Z\le 0 \quad (18)$$

Considering the effect of moisture in the energy equation, a coefficient F(M, φ_u) is multiplied to the solution of energy equation. This coefficient is obtained via comparing the adiabatic temperature of dry dust flame with a dust flame which has moisture content. Consequently F(M, φ_u)≤1 and

$$\theta^0=F(M,\phi_u)\exp(Z)$$
$$Z=\frac{\ln(\theta^0)}{F(M,\phi_u)}\rightarrow Z_d=\frac{\ln(\theta^0{}_d)}{F(M,\phi_u)} \quad (19)$$

4. 2. Heating Subzone (-∞<Z<Z_d) Mass conservation equation of organic particles:

$$\frac{dy_s}{dZ}=0$$
$$Z=-\infty\rightarrow y_s=\frac{Y_{Fu}+Y_{H_2ORu}}{Y_{FC}}=\alpha \quad (20)$$
$$\rightarrow y_s=\alpha$$

Y_{Fu} and Y_{H_2ORu} in the above equation are the amount of available fuel and moisture in initial particles respectively. Conservation equation of gaseous fuel:

$$\frac{dy_F}{dZ}=\frac{1}{Le}\frac{d^2y_F}{dZ^2}$$
$$\rightarrow y_F=P_1\exp(LeZ)+P_2 \quad (21)$$

4. 3. Drying Subzone $(Z_d<Z<Z_{vap})$ Mass conservation equation of organic particles:

$$\frac{dy_s}{dZ}=-\gamma y_s^{\frac{2}{3}}(F(M,\phi_u)\exp(Z))^n$$
$$Z=Z_d\rightarrow y_s=\alpha$$
$$Z=Z_{vap}\rightarrow y_s=\frac{Y_{Fu}}{Y_{FC}}=\alpha' \quad (22)$$
$$\rightarrow y_s=[\frac{-\gamma_1}{3n}(F(M,\varphi_u))^n\exp(nz)+\frac{\gamma_1}{3n}(F(M,\varphi_u))^n\exp(nZ_d)+\alpha^{1/3}]^3$$

By defining $a_1=\gamma_1/3n$ the upper equation changes to below equation:

$$\rightarrow y_s=(-a_1(F(M,\varphi_u))^n\exp(nZ)+a_1(F(M,\varphi_u))^n\exp(nZ_d)+\alpha^{1/3})^3 \quad (23)$$

To obtain explicit expression of Z_{vap}:

$$\alpha'=[-a_1(F(M,\phi_u))^n\exp(nZ_{vap})+a_1(F(M,\phi_u))^n\exp(nZ_d)+\alpha^{1/3}]^3$$
$$\rightarrow Z_{vap}=\frac{1}{n}\ln\left(\frac{(F(M,\phi_u))^n\exp(nZ_d)+\frac{\alpha^{1/3}-\alpha'^{1/3}}{a_1}}{(F(M,\phi_u))^n}\right) \quad (24)$$

Conservation equation of gaseous fuel:

$$\frac{dy_F}{dZ}=\frac{1}{Le}\frac{d^2y_F}{dZ^2}$$
$$\rightarrow y_F=P_3\exp(LeZ)+P_4 \quad (25)$$

4. 4. Volatile Evaporation Subzone $(Z_{vap}<Z<0)$ Mass conservation equation of organic particles:

$$\frac{dy_s}{dZ} = -\gamma_2 y_s^{\frac{2}{3}} \theta^{0n} \times H(Z - Z_{vap})$$
$$Z = Z_{vap} \rightarrow y_s = \alpha'$$
$$Z = 0 \rightarrow y_s = finite \quad (26)$$

$$\rightarrow y_s = [\frac{-\gamma_2}{3n}(F(M,\varphi_u))^n \exp(nz) + \frac{\gamma_2}{3n}(F(M,\varphi_u))^n \exp(nZ_{vap}) + \alpha^{1/3}]^3$$

By defining $a_2=\gamma_2/3n$ upper equation changes to below:

$$y_s = [-a_2(F(M,\varphi_u))^n \exp(nZ) + a_2(F(M,\varphi_u))^n \exp(nZ_d) + (\alpha')^{1/3}]^3 \quad (27)$$

Conservation equation of gaseous fuel:

$$\frac{dy_F}{dZ} = \frac{d^2 y_F}{dZ^2} + \gamma_2 y_s^{\frac{2}{3}} \theta^{0n} \times H(Z - Z_{vap})$$
$$\rightarrow y_F = \frac{A.Le}{n(n - Le)} \exp(nZ) + \frac{B.Le}{2n(2n - Le)} \exp(2nZ) + \frac{C.Le}{3n(3n - Le)} \exp(3nZ) + P_5 \exp(Le.Z) + P_6 \quad (28)$$

By solving gaseous fuel conservation equation in all three subzones according to the boundary conditions mentioned below, it is possible to determine all of the six constants which are revealed in their solutions.

$$Z = -\infty \rightarrow y_F = 0$$
$$Z = Z_d \rightarrow \left\{ y_F\Big|_{Z_d^-} = y_F\Big|_{Z_d^+}, , , \frac{dy_F}{dZ}\Big|_{Z_d^-} = \frac{dy_F}{dZ}\Big|_{Z_d^+} \right. \quad (29)$$
$$Z = Z_{vap} \rightarrow \left\{ y_F\Big|_{Z_{vap}^-} = y_F\Big|_{Z_{vap}^+}, , , \frac{dy_F}{dZ}\Big|_{Z_{vap}^-} = \frac{dy_F}{dZ}\Big|_{Z_{vap}^+} \right.$$
$$Z = 0 \rightarrow y_{F=} y_{F_f} = 0$$

4. 5. Reaction Zone ($Z = 0$) In this zone, the rate of reaction is considerable and convection and devolatilization terms are negligible in comparison with diffusion and reaction terms (asymptotic solution $\varepsilon \rightarrow 0$). It means:

$$\frac{d\theta^0}{dZ} \approx 0, , , \frac{dy_F}{dZ} \approx 0, , , \gamma y_s^{\frac{2}{3}} \theta^{0n} \approx 0 \quad (30)$$

Governing equations in this zone transform to:

$$\frac{dy_s}{dZ} = 0 \rightarrow y_s = cte$$
$$\frac{d^2\theta^0}{dZ^2} = -\omega_F \frac{\rho_u}{\rho} \quad (31)$$
$$\frac{1}{Le}\frac{d^2 y_F}{dZ^2} = \omega_F \frac{\rho_u}{\rho}$$

In the above equation, gaseous fuel reaction [16] is defined as:

$$w_F = \nu_F W_F k_F C_F$$
$$k_F = B_F \exp(-\frac{E_F}{RT}) \quad (32)$$

The subscript F denote gas C, W and k are the molar concentration, molecular weight and the rate constant of the overall reaction; v is stoichiometric coefficient of the fuel component which can be substituted by relevant gas yield in devolatilization process.

Expansion parameter $\varepsilon=1/Ze$ is used to analyze the flame structure in reaction zone, and to define following parameters:

$$\eta = \frac{Z}{\varepsilon} \quad y = \frac{y_F - y_{F\,F}}{\varepsilon} \quad t == \frac{1-\theta^0}{\varepsilon} \quad (33)$$

Thus:

$$\begin{cases} \frac{d^2 t}{d\eta^2} = \varepsilon \omega_F \frac{\rho_u}{\rho} \\ \frac{1}{Le}\frac{d^2 y}{d\eta^2} = \varepsilon \omega_F \frac{\rho_u}{\rho} \end{cases} \rightarrow \frac{d^2(t - \frac{1}{Le} y)}{d\eta^2} = 0 \quad (34)$$

Hence, t=y/Le.

By substituting the relevant quantities, they yield to:

$$\frac{d^2 t}{d\eta^2} = \Lambda(y + \frac{y_F}{\varepsilon}) \exp(-t)$$
$$\Lambda = \frac{\varepsilon^2}{V_u^2}\left[\frac{Le\lambda_u \nu_F B_F}{\rho_u C} \exp\left(-\frac{E}{RT_f}\right)\right] \quad (35)$$

By solving the above equation in reaction zone according to these boundary conditions:

$$\eta \rightarrow +\infty \quad \frac{dt}{d\eta} = \frac{dy}{d\eta} = 0$$
$$\eta \rightarrow -\infty \quad \frac{dt}{d\eta} = -F(M, \phi_u) \quad (36)$$

By introducing new variables and their related boundary conditions, it is possible to solve Equation (35) as below:

$$\frac{dt}{d\eta} = p$$
$$\eta \rightarrow -\infty \begin{cases} p = -F(M,\phi_u) \\ t = +\infty \end{cases}$$
$$\eta \rightarrow +\infty \begin{cases} p = 0 \\ t = 0 \end{cases} \quad (37)$$
$$pdp = \Lambda\langle b\exp(-t) + t\exp(-t)\rangle$$

Thus:

$$(F(M, \phi_u))^2 = 2\Lambda(b + 1) \quad (38)$$

$$V_u^2 = \frac{2Le(1+b)\nu_F \lambda_u B_F \varepsilon^2}{\rho_u C(F(M,\phi_u))^2} \exp(-\frac{E}{RT_f})$$

The matching condition across the reaction zone is used to obtain another expression for determination of T_f.

$$\left[\frac{dy_F}{dZ}\right]_{0^-} + \left[\frac{d\theta^0}{dZ}\right]_{0^-} = \left[\frac{dy_F}{dZ}\right]_{0^+} + \left[\frac{d\theta^0}{dZ}\right]_{0^+} \quad (39)$$

For sufficiently high values of T_f, it is reasonable to set $Y_{FF=0}$, which implies that b=0. By assuming that the gradients at 0^+ are of the order of ε, it results to:

$$F(M,\phi_u) + \left(\frac{A.Le}{(n-Le)} + \frac{B.Le}{(2n-Le)} + \frac{C.Le}{(3n-Le)} + P_5 Le\right) = 0 \quad (40)$$

By solving Equations (38) and (40) simultaneously, it is possible to achieve flame characteristics.

5. RESULTS

The structure of premixed flames propagating in a uniform cloud of organic fuel particles is considered. Explicit algebraic equations are obtained for predicting the burning velocity of the flame as a function of the initial size and number density of the particles.

For φ_u>1, the equivalence ratio based on the fuel available in the initial fuel particles and the final adiabatic temperature can be calculated:

$$\varphi_u = \frac{274.56}{16(1-Y_{Fu})-18MY_{Fu}} Y_{Fu}$$

$$C(T_b - T_u) = \frac{\nu_{CH_4} M_{CH_4} Q - \nu_{H_2O} M_{H_2O} Q_{dry}}{\nu_{O_2} M_{O_2}} Y_{O_{2_u}}$$

In the above equations, Q is heat released per unit mass of gas fuel consumed and Q_{dry} is latent heat (h_{fg}) of H_2O per unit mass. The chemical and thermo-physical characteristics of presumed fuel is listed in Table 1.

To evaluate the presented model accuracy, flame temperature is compared with the experimental data calculated by Proust [21]. As shown in Figure 2, the evolution of flame temperature as a function of mass particle concentration is in reasonable agreement with the experimental data.

In gas flame analysis, we deal with two resistances against flame propagation, heat transfer resistance and combustion resistance. In dry dust flame propagation, evaporation or devolatization resistance is added to those resistances. If this resistance is neglected, we can treat particles like gasses fuel. As shown in Figure 3, increase in φ_u causes a decrease in adiabatic flame temperature, because excess reactant that not contributes in reaction is increasing and these unburned reactants absorb fraction of released heat from combustion. Also, it is concluded that increase in moisture content causes adiabatic temperature to decrease, because part of combustion heat is used to vaporize moisture content.

TABLE 1. The list of Chemical and thermo-physical characteristics [16, 20]

Parameter	*Quantity*	*Unit*
Q	50009	$[Kj / Kg_{fuel}]$
Q_{dry}	2257	$[Kj / Kg_{water}]$
A	3.4×10^{-6}	$[g/(cm^2.K.s)]$
A'	3.1×10^{-5}	$[g/(cm^2.K.s)]$
n	1.33	-
λ_u	1.46×10^{-3}	$[j/(cm.s.K)]$
ρ_s	1	$[g/cm^3]$
ρ_u	1.135×10^{-3}	$[g/cm^3]$

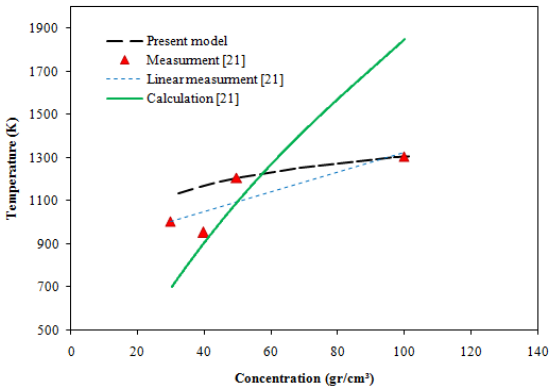

Figure 2. The variation of flame temperature as a function of mass particle concentration for both present model (Le=1, r_u=31μm and moisture content=0) and experimental data [21].

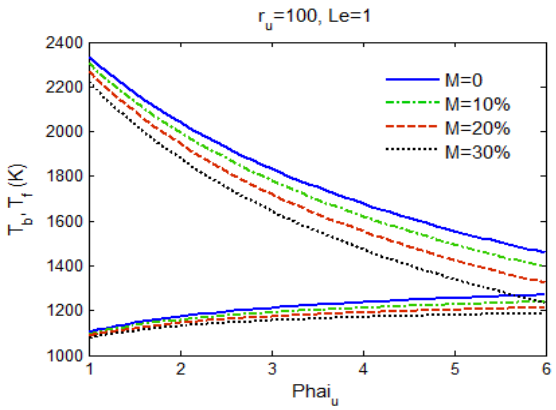

Figure 3. Adiabatic temperature T_b(K) and flame temperature T_f(K) as a function of φ_u for different moisture content

As mentioned above, in analysis of dry dust devolatization process resists against flame propagation. In wet dust, the moisture evaporation resistance additionally exists in front of flame propagation. As the moisture content in the particle becomes more, the moisture evaporation resistance increases thus the flame propagation slows down which yields to decrease in flame temperature and burning velocity as shown in Figures 3 and 4.

As shown in Figures 3 and 4, by increasing φ_u, burning velocity and flame temperature increase. Indeed, increase in equivalence ratio φ_u or particle number density causes to increase in moisture evaporation and devolatization rates. Consequently, the related resistances diminish which can enhance the flame propagation individually, so the flame temperature and burning velocity should enhance. The flame temperature in Figure 3 and burning velocity in Figure 4 are presented for r_u=100μm with different moisture contents.

As shown in Figure 5, the boundary condition $Z = 0^- \rightarrow y_F = y_{FF} = 0$ causes a peak in the mass fraction of gaseous fuel (Y_F) in preheat zone, while there is no peak for Y_s. The minimum value of Y_s occurs at $Z = 0^-$.

In Figures 6, 7 and 8, the effect of moisture content on the mass fraction of gas Y_F and particle Y_s are illustrated. In these Figures, it is considered that φ_u =1 and r_u=100μm. From these graphs, it is concluded that when the moisture content increases, the mass fraction of gas in constant non-dimensional distance (Z) decreases. On the other hand, increase in moisture content causes an increase in mass fraction of particle Y_s in heating and drying subzones, but in volatile evaporation subzone effect of moisture content is completely reverse.

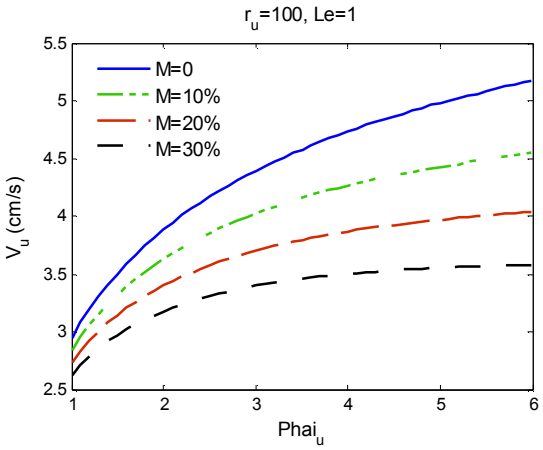

Figure 4. Burning velocity V_u (cm/s) as a function of φ_u for different moisture content.

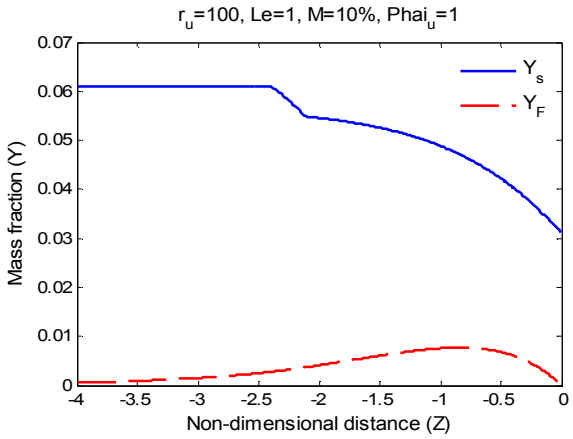

Figure 5. Mass fraction of gas Y_F and particle Y_s as a function of non-dimensional distance (Z).

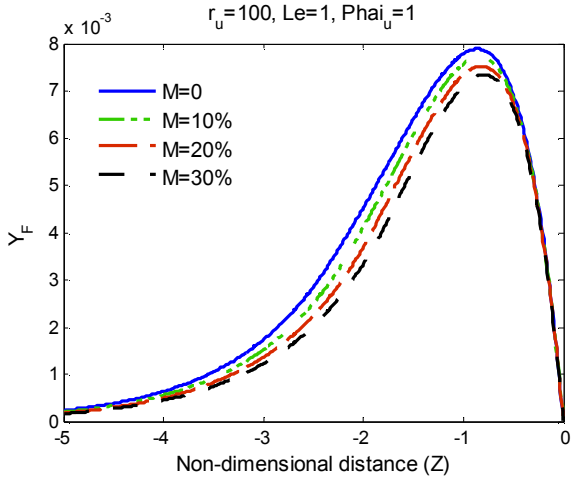

Figure 6. Mass fraction of gas Y_F as a function of non-dimensional distance (Z) for different moisture content.

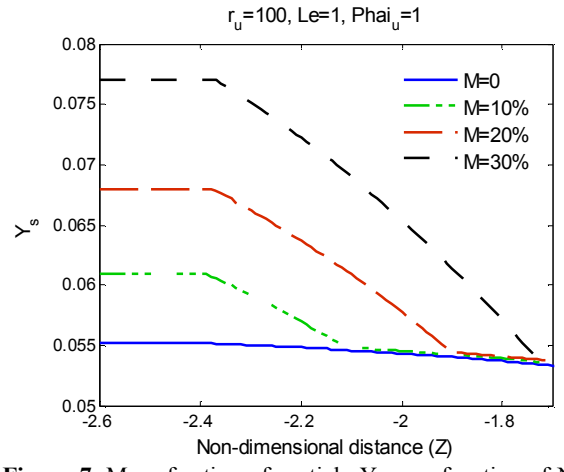

Figure 7. Mass fraction of particle Y_s as a function of Non-dimensional distance (Z) for different moisture content in heating and drying subzone.

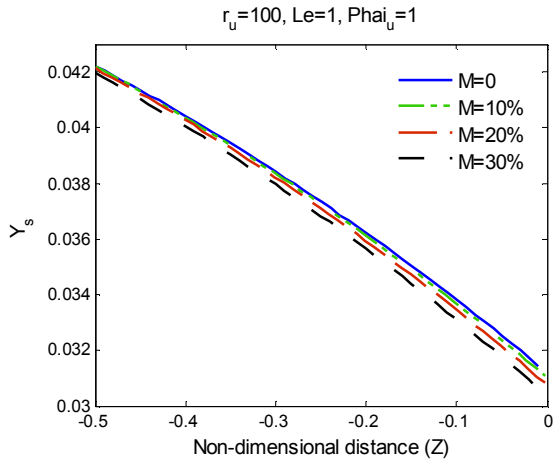

Figure 8. Mass fraction of particle Y_s as a function of Non-dimensional distance (Z) for different moisture content in volatile evaporation subzone.

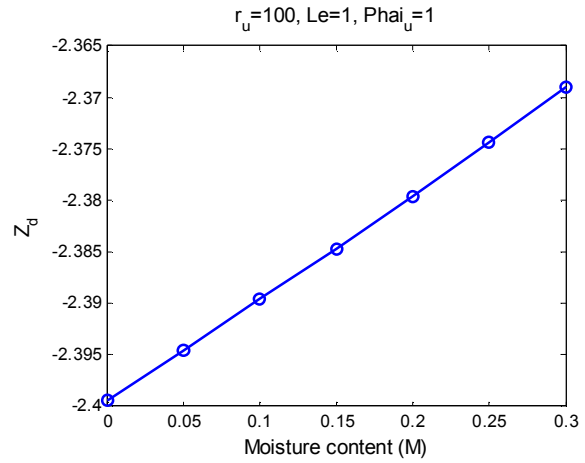

Figure 9. Moisture evaporation initiation point (Z_d) as a function of moisture content (M).

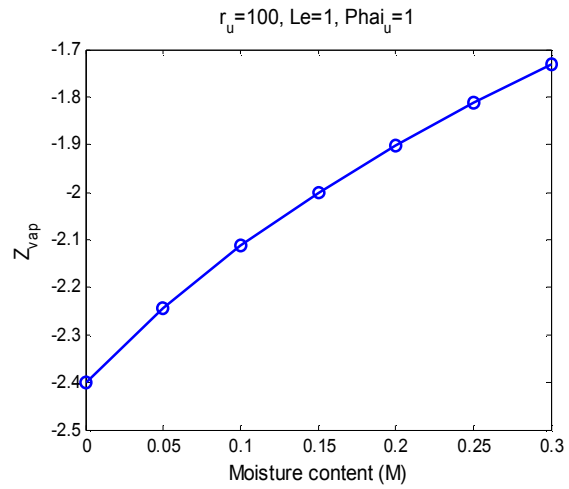

Figure 10. Moisture evaporation end point (Z_{vap}) as a function of moisture content (M).

As shown in Figure 7, it is concluded that increase in moisture content causes an increase in mass fraction. This may be is understood according to below equation:

$$Y_s = \frac{m_{CH_4} + m_{H_2O}}{m_{O_2} + m_{N_2} + m_{CH_4} + m_{H_2O}}$$

In the drying and heating subzones, presence of moisture yields to higher mass fraction Y_s, but in the volatile evaporation subzone, there is no moisture in the particle. In other words, by omitting H_2O from numerator of the above equation, denominator of equation does not change. Hence, for volatile evaporation subzone which is shown in Figure 8, mass fraction (Y_s) of wetter particle becomes less than that of the drier one. Clearly, the moisture content can affect the drying subzone, both the initial point and the end point. As it can be seen in Figure 9, increase in moisture content causes the moisture evaporation initiation point (Z_d) to move toward the reaction zone. It is the result of flame temperature reduction which causes T_d=373K to occur at closer point to the flame zone. In addition, according to Equation (19), Z_d is a function of T_f and increase in moisture content yields increase in Z_d.

Evidently, the moisture content can change the drying end point more than the drying initiation point. This is also concluded from Equation (24) (Z_{vap} have an intense dependency on moisture content). As shown in Figure 10, Z_{vap} moves toward reaction zone by increasing in moisture content. By subtracting Z_d from Z_{vap} in Figures 9 and 10, it is deduced that increasing the moisture content causes the drying subzone to lengthen, which is expectable. Also, in a higher moisture contents, the vaporization length get thinner and produced gaseous fuel become less. Lewis number variation (the ratio of thermal diffusivity to mass diffusivity) has a strong effect on the flame temperature and burning velocity.

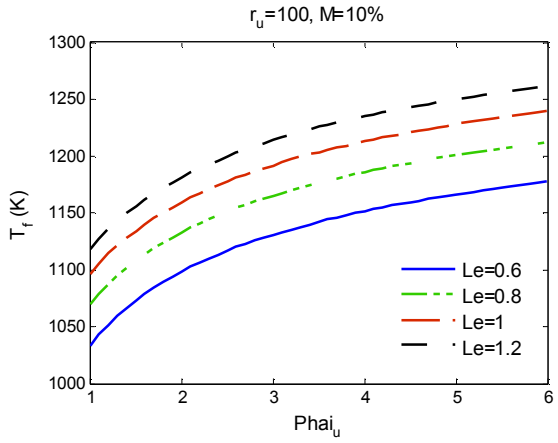

Figure 11. Flame Temperature as a function of φ_u for different Lewis numbers.

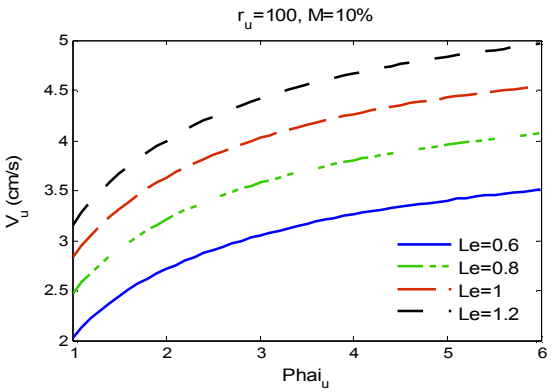

Figure 12. Burning velocity V_u (cm/s) as a function of φ_u for different Lewis numbers.

Increasing Le associates with the noticeable rise in the thermal diffusivity which improves the combustion condition. Improvement in combustion phenomenon causes increase in flame temperature and burning velocity which is shown in the Figures 11 and 12.

6. CONCLUSION

In this article, the structure of moist lycpodium dust flame has been investigated. Combustion of organic particle is composed of heating, drying, devolatization and burning processes. Since the particle size is small here, these processes do not take place simultaneously. In diffusion control flame with large Zeldovich number, the flame structure is divided into three zones: preheat, reaction and convection. In the preheat zone, particles are heated in heating subzone upto T_d=273K, and then drying process starts in drying subzone where all moisture content of the particles comes out. In devolatization process which begins at the end of the drying process (volatile evaporation subzone), particles vaporize to yield a gaseous fuel and finally, the produced gas burns in the reaction zone. The results indicate that the moisture resists against flame propagation, thus increase in particle moisture content yields to decrease in flame temperature and burning velocity. Also, increase in equivalence ratio (φ_u) or increase in Lewis number causes in moisture evaporation and devolatization rates to increase, and consequently both flame temperature and burning velocity increase.

7. REFERENCES

1. Yang, Y., Sharifi, V. and Swithenbank, J., "Effect of air flow rate and fuel moisture on the burning behaviours of biomass and simulated municipal solid wastes in packed beds", ***Fuel***, Vol. 83, No. 11, (2004), 1553-1562.
2. Mohan, D., Pittman, C. U. and Steele, P. H., "Pyrolysis of wood/biomass for bio-oil: a critical review", ***Energy & Fuels***, Vol. 20, No. 3, (2006), 848-889.
3. Di Blasi, C., "Modeling chemical and physical processes of wood and biomass pyrolysis", ***Progress in Energy and Combustion Science***, Vol. 34, No. 1, (2008), 47-90.
4. Parikh, J., Channiwala, S. and Ghosal, G., "A correlation for calculating HHV from proximate analysis of solid fuels", ***Fuel***, Vol. 84, No. 5, (2005), 487-494.
5. Zhao, W., Li, Z., Zhao, G., Zhang, F. and Zhu, Q., "Effect of air preheating and fuel moisture on combustion characteristics of corn straw in a fixed bed", ***Energy Conversion and Management***, Vol. 49, No. 12, (2008), 3560-3565.
6. Chao, C. Y., Kwong, P. C., Wang, J., Cheung, C. and Kendall, G., "Co-firing coal with rice husk and bamboo and the impact on particulate matters and associated polycyclic aromatic hydrocarbon emissions", ***Bioresource technology***, Vol. 99, No. 1, (2008), 83-93.
7. Hurt, R. H., "Structure, properties, and reactivity of solid fuels", in Symposium (International) on Combustion, Elsevier. Vol. 27, No. Issue, (1998), 2887-2904.
8. Vijayaraghavan, G., "Impact assessment, modelling, and control of dust explosions in chemical process industries", ***MTech Thesis, Department of Chemical Engineering, Coimbatore Institute of Technology***, Vol., No., (2004.(
9. Abbasi, T. and Abbasi, S., "Dust explosions–Cases, causes, consequences, and control", ***Journal of Hazardous Materials***, Vol. 140, No. 1, (2007), 7-44.
10. Eckhoff, R., "Dust explosions in the process industries: identification, assessment and control of dust hazards, Gulf professional publishing, (2003).
11. Proust, C., "A few fundamental aspects about ignition and flame propagation in dust clouds", ***Journal of Loss Prevention in the Process Industries***, Vol. 19, No. 2, (2006), 104-120.
12. Proust, C., "Dust explosions in pipes: a review", ***Journal of Loss Prevention in the Process Industries***, Vol. 9, No. 4, (1996), 267-277.
13. Pilao, R., Ramalho, E. and Pinho, C., "Influence of initial pressure on the explosibility of cork dust/air mixtures", ***Journal of Loss Prevention in the Process Industries***, Vol. 17, No. 1, (2004), 87-96.
14. Pilao, R., Ramalho, E. and Pinho, C., "Explosibility of cork dust in methane/air mixtures", ***Journal of Loss Prevention in the Process Industries***, Vol. 19, No. 1, (2006), 17-23.
15. Steen, H., "Handbuch des Explosionsschutzes, John Wiley & Sons, (2012)
16. Seshadri, K., Berlad, A. and Tangirala, V., "The structure of premixed particle-cloud flames", ***Combustion and flame***, Vol. 89, No. 3, (1992), 333-342.
17. Bidabadi, M. and Rahbari, A., "Modeling combustion of lycopodium particles by considering the temperature difference between the gas and the particles", ***Combustion, Explosion, and Shock Waves***, Vol. 45, No.30, (2009) 278-285
18. Bidabadi, M. and Rahbari, A., "Novel analytical model for predicting the combustion characteristics of premixed flame propagation in lycopodium dust particles", ***Journal of mechanical science and technology***, Vol. 23, No. 9, (2009,) 2417-2423.
19. Bidabadi, M., Shakibi, A. and Rahbari, A., "The radiation and heat loss effects on the premixed flame propagation through lycopodium dust particles", ***Journal of the Taiwan Institute of Chemical Engineers***, Vol. 42, No. 1, (2011), 180-185.

20. Han, O.-S., Yashima, M., Matsuda, T., Matsui, H., Miyake, A., and Ogawa, T., "Behavior of flames propagating through lycopodium dust clouds in a vertical duct", ***Journal of Loss Prevention in the Process Industries***, Vol. 13, No. 6, (2000), 449-457.

21. Proust, C., "Flame propagation and combustion in some dust-air mixtures", ***Journal of Loss Prevention in the Process Industries***, Vol. 19, No. 1, (2006), 89-100.

An Analytical Model for Flame Propagation through Moist Lycopodium Particles with Non-unity Lewis Number

M. Bidabadi [a], S. A. Mostafavi [b], F. Faraji Dizaji [a], H. Beidaghy Dizaji [a]

[a] *Department of Mechanical Engineering, Iran University of Science and Technology, Tehran, Iran*
[b] *Department of Mechanical Engineering, Faculty of Engineering, Arak University, Iran*

P A P E R I N F O

Paper history:
Received 21 November 2012
Received in revised form 15 September 2013
Accepted 21 January 2014

Keywords:
Analytical Model
Lycopodium particle
Moisture content
Lewis number
Flame Temperature
Burning Velocity

چکیده

در تحقیق فوق برای انتشار شعله در ابر یکنواختی از ذرات ارگانیک از یک ساختار یک‌بعدی استفاده شده است که در آن ساختار شعله به سه ناحیه تقسیم‌بندی می‌شود. ناحیه‌ی پیش‌گرم اولین ناحیه است که خود ای به سه زیرناحیه تقسیم می‌شود. در زیرناحیه‌ی اول (گرمایش) ذره حرارت دریافت می‌کند تا به دمای تبخیر رطوبت برسد. در زیرناحیه‌ی بعدی (خشک شدن) رطوبت ذره تبخیر می‌شود و در زیرناحیه‌ی آخر عمل پیرولیز اتفاق می‌افتد. ناحیه‌ی دوم ناحیه احتراق بوده و در آخر، ناحیه‌ی پس از شعله قرار دارد. در این پژوهش از یک روش تحلیلی برای حل معادلات حاکم بر احتراق ذرات در نواحی فوق استفاده شده است. بررسی کلی از این مطالعه منجر به یک رابطه‌ی غیر خطی برای سرعت سوزش می‌گردد. در نهایت، نتایج به دست آمده نشان می‌دهد که کاهش مقدار رطوبت یا افزایش نسبت هم‌ارزی و عدد لوئیس باعث افزایش در نرخ‌های تبخیر رطوبت و پیرولیز شده و در نتیجه دمای شعله و سرعت سوزش افزایش می‌یابد.

doi: *10.5829/idosi.ije.2014.27.05b.16*